ELSEVIER

Structure and electrochemical characterization of $Li_{1+x}Mn_{2-x}O_4$ spinels for rechargeable lithium batteries

Toshimi Takada [a,*], Hiroshi Hayakawa [a], Hirotoshi Enoki [a], Etsuo Akiba [a], Helen Slegr [b], Isobel Davidson [b], John Murray [b]

[a] *National Institute of Materials and Chemical Research, Ibaraki 305-8565, Japan*
[b] *Institute for Chemical Process and Environmental Technology, National Research Council, Canada*

Abstract

Neutron and X-ray powder diffraction and Rietveld refinements have been carried out for the well-crystallized samples with a homogeneous composition $Li_{1+x}Mn_{2-x}O_4$ $(0 \leq x \leq 0.125)$. The lattice parameter of these spinels changes with both the composition and the synthesis temperature. SEM and TEM micrographs show that the crystallites appear as single crystals with a size of 0.1–2 μm. The phase transition from cubic $Fd\bar{3}m$ to orthorhombic $Fddd$ around 280 K of samples $Li_{1+x}Mn_{2-x}O_4$ $(x \leq 0.04)$ was observed using low temperature XRD and DSC. The orthorhombic phase further converts to a single tetragonal phase $I4_1/amd$ around 65 K. The charge/discharge capacity, and cyclability of these samples were examined in both the 3 V and the 4 V regions. We found that the discharge capacity as well as the cyclability of the cell $Li/Li_{1+x}Mn_{2-x}O_4$ change largely with not only the value of x but also the crystal structure which depends on the synthesis conditions. © 1999 Elsevier Science S.A. All rights reserved.

Keywords: Lithium; Battery; $Li_{1+x}Mn_{2-x}O_4$

1. Introduction

The high energy density and good cycle life of commercial lithium ion batteries make them very attractive for use in energy storage and in powering emission free vehicles in the near future. In order to overcome the resource limitation and thus the high cost of Co, Li–Mn–O spinels are being studied extensively as a replacement for $LiCoO_2$.

Research [1–3] indicates that the spinel lattice parameter varies with both the composition and the synthesis conditions of the solid-state reactions, but such information was limited to samples $Li_{1+x}Mn_{2-x}O_4$ prepared under certain conditions. The composition uncertainty inside each crystallite remains to be considered. On the other hand, many reports [4–6] dealt with the low temperature synthesis processes using the solution techniques which possess the advantage of homogeneity of the spinel composition and control of the grain size over the solid-state reactions. The main problem with such low temperature processes is how to ensure the crystallinity of the particles in order to

obtain decent electrode performance. Systematic crystallographic studies of samples synthesized under various conditions are indispensable to understand the differences in the electrode performance of Li–Mn–O spinels.

In this study, a new synthesis process has been developed to obtain well-crystallized lithium manganese oxide spinels with a homogenous composition $Li[Li_xMn_{2-x}]O_4$ $(0 \leq x \leq 0.125)$. Rietveld refinements using both the X-ray and neutron diffraction data, and low-temperature DSC measurements were conducted to clarify the relations between the spinel lattice parameter, the lattice stability, the spinel composition, and the synthesis conditions. The electrode performance of these samples was examined using the cell $Li/Li[Li_xMn_{2-x}]O_4$ in both the 3 V and the 4 V regions.

2. Experimental

2.1. Synthesis of well-crystallized Li–Mn–O spinels

A value 99.9% pure lithium acetate $LiOAc \cdot 2H_2O$, and manganese nitrate $Mn(NO_3)_2 \cdot 6H_2O$ (from Wako) were used as starting materials. The raw materials with a molar

ratio of Li/Mn 1/2–3/5 ($0.0 \leq x \leq 0.125$) were first heated at 100°C to obtain a uniform solution, and then slowly oxidized around 250°C under flowing O_2 to convert the solution to a solid Li–Mn–O precursor. The precursor was then ground and pelletized (10 mm in the diameter and height) before heating first at 650°C and then at 800°C for 1 day each. The 900°C-samples were obtained by reheating the 800°C-samples at 900°C for 1 day. All the heat-treatments were conducted under 200 ml/min flowing oxygen and cooling rate was 1°C/min. Details of the preparation process were described in our previous reports [7,8].

2.2. Characterization

X-ray powder diffraction data were collected between $2\theta = 15°–120°$ with a step interval of 0.02° at room temperature on a Rigaku RAX-I X-ray diffractometer with monochromatized Cu–Kα radiation ($\lambda = 1.5406$ Å) at 40 kV, 30 mA. Structural refinements were carried out with a Rietveld refinement program, *RIETAN-97* β-version [9]. Scanning electron micrographs were taken at room temperature on a Hitachi S-800 microscope equipped with a field emission gun, at 10 kV. TEM was taken with a JEOL/JEM 1200 FXII at room temperature.

2.3. Electrode performance

The charge/discharge capacity and cyclability were evaluated using the 2430 coin cell Li/Li[Li$_x$Mn$_{2-x}$]O$_4$, using Li metal as negative and reference electrodes, and 1.0 M LiPF$_6$ dissolved in ethylene carbonate (EC) and dimethyl carbonate (DMC) (1:1 in volume) as the electrolyte. The composite electrode was made by mixing the spinel powders with 30.0 wt.% acetylene black and 4.0 wt.% of polyvinylidene fluoride (PVDF) dissolved in 1-methyl-2-pyrrolidone (NMP). The slurry was pressed onto an aluminum mesh current collector and dried at 120°C under vacuum.

3. Results and discussion

3.1. Synthesis and structural changes of Li–Mn–O spinels

Fig. 1 shows the typical SEM pictures of the spinel Li$_{1+x}$Mn$_{2-x}$O$_4$ crystallites in the samples with a Li/Mn = 3/5 ($x = 0.125$). At temperatures below 800°C, the size of the crystallites were rather uniform with a range of 0.1 to 0.3 μm. At higher temperatures, well-developed polyhedra (mainly octahedra bounded by eight (111) planes, were clearly observed, and the size of the crystallites increased to 1–2 μm in the 900°C-samples. Fig. 2 shows a typical electron diffraction pattern of one LiMn$_2$O$_4$ ($x = 0.0$, 900°C-sample). Obviously, the particles are well-crystallized as a single crystal which possesses a typical $Fd\bar{3}m$ cubic spinel structure.
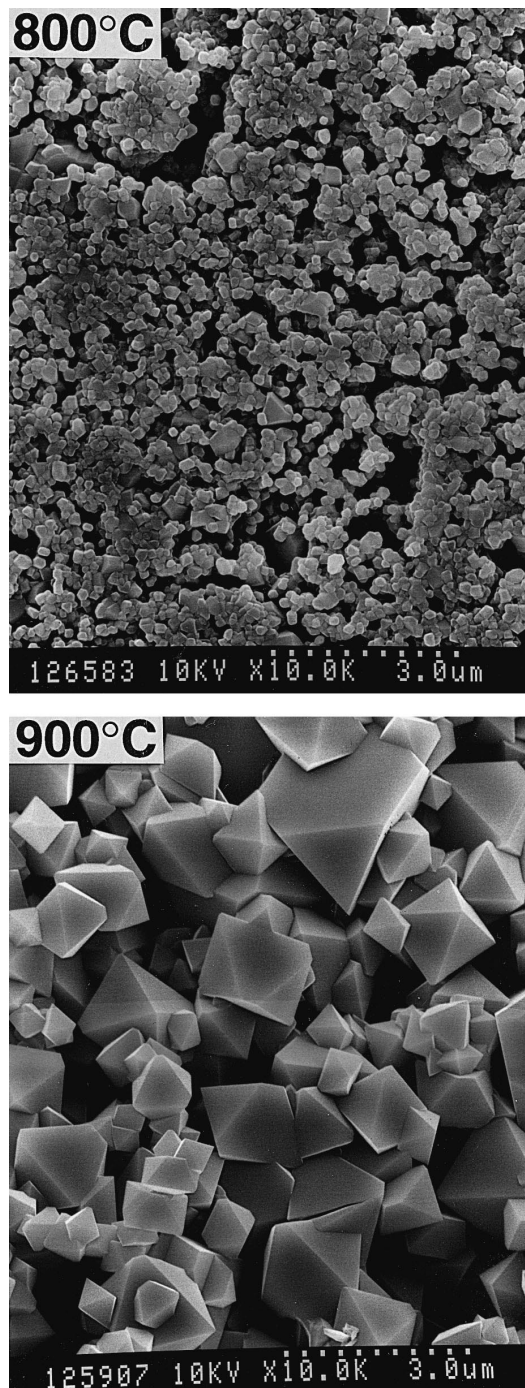

Fig. 1. Typical SEM micrographs for the spinel Li$_{1+x}$Mn$_{2-x}$O$_4$ samples ($x = 0.125$).

Rietveld refinements were carried out for all samples synthesized at both 800 and 900°C using the space group $Fd\bar{3}m$. Details of the procedure are described in our previous reports [9,10]. The refined lattice parameter a is plotted in Fig. 3 against x in Li$_{1+x}$Mn$_{2-x}$O$_4$. The lattice parameters for the 800°C-samples obtained from both X-ray and neutron diffraction data are in strict consistence, and decreases linearly as the Li content increases. For the 900°C-samples which obtained by reheating the exactly the
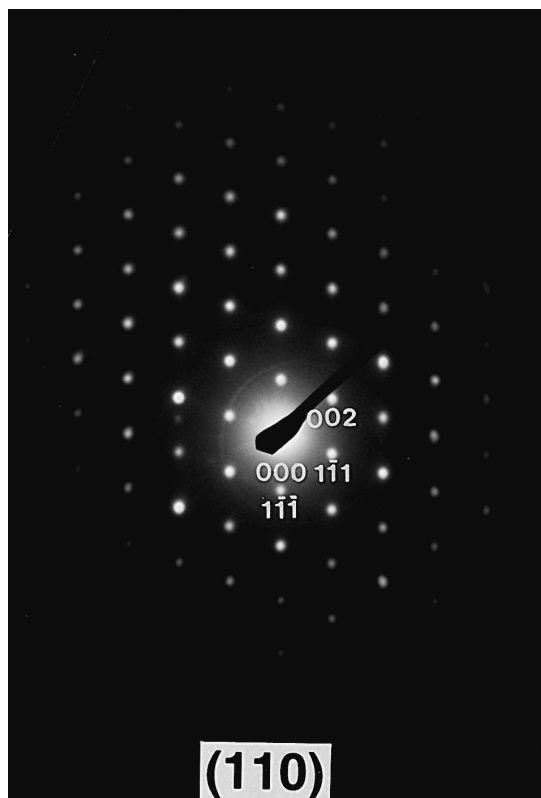
Fig. 2. Electron diffraction pattern of one crystallite in the 900°C-LiMn$_2$O$_4$ sample ($x = 0.0$).

Fig. 4. Structural phase diagram of spinel LiMn$_2$O$_4$ at temperatures 10–350 K.

same 800°C-samples, the lattice parameters change largely and reach a maximum around 8.246 Å, which clearly indicates the variation of the spinel composition. Losing of Li at 900°C could be the cause and the composition analysis is in progress.

3.2. Structural phase transitions of LiMn$_2$O$_4$

With careful study on the X-ray powder diffraction profiles for a well-crystallized LiMn$_2$O$_4$ ($x = 0.0$) sample
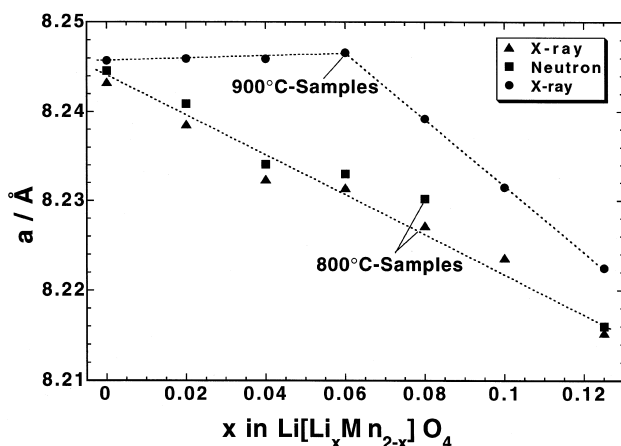

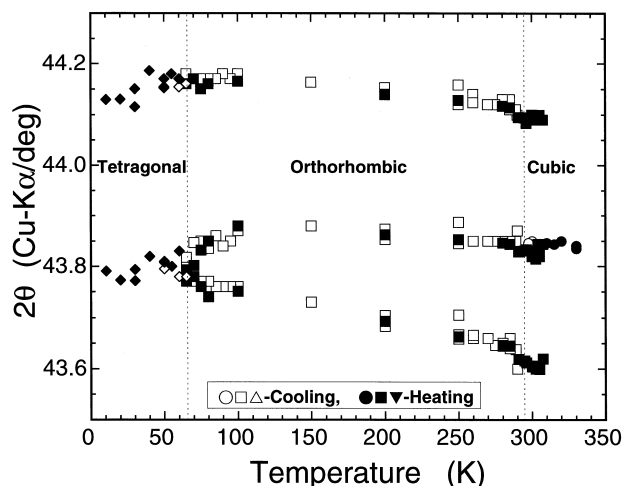Fig. 3. Plot of the lattice parameter against the lithium content x in Li$_{1+x}$Mn$_{2-x}$O$_4$.

at temperatures 10–350 K, we found that the low-temperature phase of LiMn$_2$O$_4$ at temperatures ranging from 280 to 70 K, is a single orthorhombic phase, and this phase further converts to a single tetragonal phase around 65 K (Fig. 4). A thermal hysteresis of 20 K was observed for the structural phase transition cubic $Fd\bar{3}m$ ⇔ orthorhombic $Fddd$, but no thermal hysteresis was detected for the second transition between the orthorhombic $Fddd$ and the tetragonal phase $I4_1/amd$. Both X-ray diffraction data and DSC curves (120–350 K) confirmed that Li rich spinels Li$_{1+x}$Mn$_{2-x}$O$_4$ ($x \leq 0.04$) showed similar phase transitions, but the degree of the structural changes decreases as the Li content x increases, and finally it disappears when x reaches 0.06. Coincidentally, it agrees well with the electrode performance of Li/Li$_{1+x}$Mn$_{2-x}$O$_4$ cells in the 4 V region, which indicates the importance of the spinel lattice stability. The cause of these phase transitions is not clear yet. The details will be reported separately [11].

3.3. Electrochemical characterization

The charge–discharge profiles and the cyclability were examined for the typical 800 and 900°C samples of Li$_{1+x}$Mn$_{2-x}$O$_4$ with x from 0.0 to 0.125. The results for 800°C samples are shown in Fig. 5. In the 4 V region, voltage plateaus were observed between 4.1 and 3.8 V, the discharge capacity decreased as x increased from 0.0 to 0.125. Also, for samples with $x \geq 0.06$, the voltage changed linearly from 4.1 to 4.0 V, indicating the difference in the structure changes during the discharge process between these samples. In the 3 V region, voltage plateaus were observed at 2.8 V, the discharge capacity varies with the cut-off voltage. In the region 3.6–1.5 V, samples with a higher x give larger discharge capacity. However, in the voltage range of 3.6–2.5 V, the discharge capacity varies independently with x. Apparently, the discharge process in the 3 V region is complex. For $x \geq 0.06$ samples, it seems
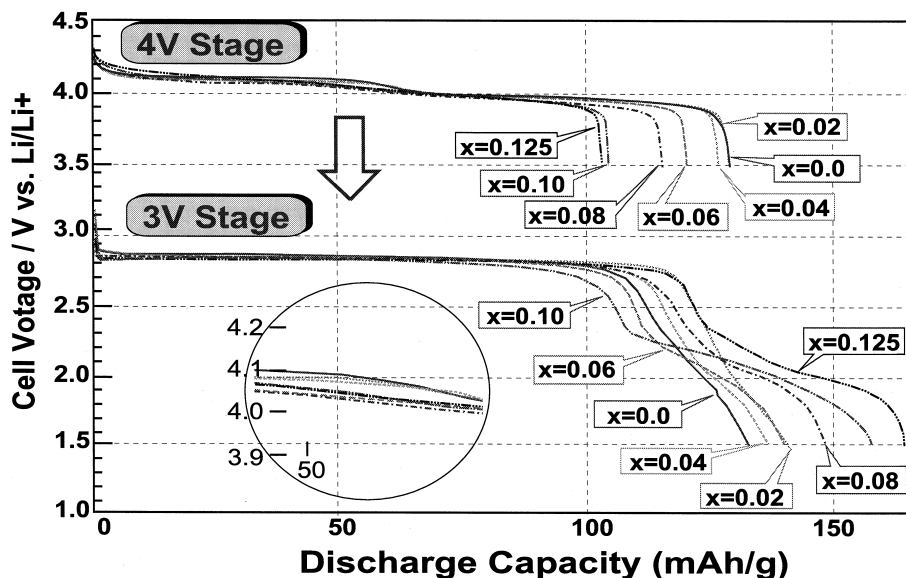
Fig. 5. First discharge profiles of the cells $Li/Li_{1+x}Mn_{2-x}O_4$ ($0.0 \leq x \leq 0.125$) in the 4 V region: 4.5–3.6 V, and in the 3 V region: 3.6–1.5 V.

that two reactions occur in the ranges 3.6–2.3 V and 2.3–1.5 V, corresponding to the two plateaus, respectively. Therefore, it would be interesting to further investigate how the structure of these samples changes during the discharge process in both the 3 V and the 4 V regions.

Good cyclability of the discharge capacity was obtained for 800°C samples in the 4 V region except for the $LiMn_2O_4$ sample ($x = 0.0$) as shown in Fig. 6. The cycling stability increases with x. A stable discharge capacity of 120 mAh/g for $0.04 \leq x \leq 0.08$ samples or 100 mAh/g for higher x samples up to 0.125, was obtained in

the 4 V region. In the 3 V region, however, the discharge capacity for all samples $0.0 \leq x \leq 0.125$ dropped sharply with cycling in the cell voltage range 3.6–2.5 V. Further optimizations of our experimental conditions to obtain the best capacity and cyclability of the cell $Li/Li_{1+x}Mn_{2-x}O_4$ in both the 3 V and the 4 V regions are necessary, in order to compare our results with those in literature. Similar results was obtained for 900°C samples but the capacity rate was rather low at $1/20$ C to obtain the decent electrode performance, because of the low diffusion rate of Li ions inside the large crystals of 1–2 μm. Consequently, not only the spinel composition (Li/Mn) but also the synthesis conditions which determine the structure and the Mn valency, affect the electrode performance of the spinel $Li_{1+x}Mn_{2-x}O_4$ in both the 3 V and the 4 V regions.
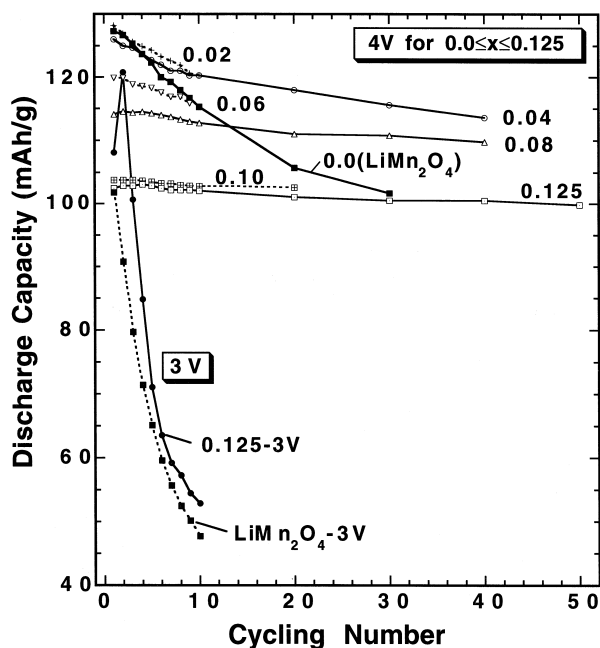
4. Conclusion

Well-crystallized $Li_{1+x}Mn_{2-x}O_4$ spinels were prepared from the stoichiometric mixture of $LiOAc \cdot 2H_2O$ and $Mn(NO_3)_2 \cdot 6H_2O$. Single-crystal-like crystallites with a size of 0.1–2.0 μm were observed. Using powder X-ray and neutron diffraction, Rietveld refinements, and low temperature DSC, we found the spinel lattice parameter varies with both the composition Li/Mn and the synthesis conditions. A new phase transition of $LiMn_2O_4$ was observed around 65 K from the orthorhombic $Fddd$ to the tetragonal phase $I4_1/amd$, which occurs after the first transition: cubic $Fd\bar{3}m \Leftrightarrow$ orthorhombic $Fddd$ around 280 K. Samples with $0.04 \leq x \leq 0.125$ showed good cyclability in the 4 V region with a rechargeable capacity of over 100 mA h/g, whereas the capacity fades abruptly in the 3 V region for all the samples with x up to 0.125. Particular attention should be given not only to the compo-

Fig. 6. Cyclability of the cell $Li/Li_{1+x}Mn_{2-x}O_4$ in the 3.0 V and the 4.0 V region.

sition (Li/Mn) but also to synthesis conditions, such as temperature and atmosphere to control Mn valency, in order to assure the spinel lattice stability and to improve the electrode performance of $Li_{1+x}Mn_{2-x}O_4$ spinels for rechargeable lithium batteries.

References

[1] R.J. Gummow, A. de Kock, M.M. Thackeray, Solid State Ionics 69 (1994) 59–67.
[2] Y. Gao, J.R. Dahn, J. Electrochem. Soc. 143 (1996) 100–114.
[3] M.M. Thackeray, M.F. Mansuetto, D.W. Dees, D.R. Vissers, Mater. Res. Bull. 31 (1996) 133–140.
[4] W. Liu, K. Kowal, G.C. Farrington, J. Electrochem. Soc. 143 (1996) 3590.
[5] Q. Zhang, A. Bonakdarpour, M. Zhang, Y. Gao, J.R. Dahn, J. Electrochem. Soc. 144 (1997) 205.
[6] Y. Lee, Y. Sun, K. Nahm, Solid State Ionics 109 (1998) 285.
[7] T. Takada, H. Hayakawa, E. Akiba, J. Solid State Chem. 115 (1995) 420–426.
[8] T. Takada, H. Enoki, H. Hayakawa, E. Akiba, J. Solid State Chem., In Press.
[9] F. Izumi, The Rietveld Method, in: R.A. Young (Ed.), Oxford Univ. Press, New York, 1993, pp. 236–253.
[10] T. Takada, H. Hayakawa, E. Akiba, F. Izumi, B. Chakoumakos, J. Solid State Chem. 130 (1997) 74–80.
[11] H. Hayakawa, T. Takada, H. Enoki, E. Akiba, J. Mater. Sci. Lett. 17 (1998) 10.